2021 7th International Conference on Advanced Computing & Communication Systems (ICACCS)

2021 7th International Conference on Advanced Computing and Communication Systems (ICACCS) | 978-1-6654-0521-8/20/$31.00 ©2021 IEEE | DOI: 10.1109/ICACCS51430.2021.9441862

Detection And Diagnosis Of Covid-19 From Chest X-Ray Images

Savarapu Lakshmi Sai Kishore[1], Achyuthuni Venkata Sidhartha[2], Pochana Srikar Reddy[3], Rahul.C.M[4], Devi Vijaya[5]
Department of Electronics and Communication Engineering,
Amrita School of Engineering, Coimbatore,
Amrita Vishwa Vidyapeetham, India
savarapukishore05@gmail.com[1], achyuthuni.venkata.sidhartha@gmail.com[2], pochanasrikarreddy@gmail.com[1],
cmrahulnambiar@gmail.com[4], v_devi@cb.amrita.edu[5]

Abstract*—The Novel Coronavirus 2019 (COVID-2019) spread quickly around the planet and turned into an undermining pandemic. The early detection of Covid disease is one of the principal challenges and needs on the planet. Early detection helps in controlling the spread of infection. Deep learning has acquired great significance in clinical picture investigation, illustrating improved performance compared to conventional machine learning framework. In this work, a DL based model is proposed for recognizing and characterizing the inconsistencies in chest X-Ray pictures and arranging as unaffected, Covid affected, or Pneumonia. Considering the information inadequacy in clinical space, VGG architecture is utilized as the pre-trained models for building the model for recognition. The quality of the X-Ray pictures and noise present in the pictures influence the decision making leading to high false positives and false negatives. In the current model, pre-processed pictures are fed as input to the DL model accomplishing a maximum accuracy of 96.56%. The proposed model outperforms the DL model without pre-processing with a false positive rate of 0.024 and a false negative rate of 0.026.

Keywords*—Covid-19, Pneumonia, Noise filtering, Deep learning, VGG Architecture, Chest X-Ray images, Convolutional Neural Network.

I. INTRODUCTION

The primary instance of Covid-19 was recorded on December 31, 2019. It spread quickly and turned into a pandemic [1]. The virus of Covid-19 is named SARS-CoV-2. The infection spread across all the mainlands and caused death to many human beings, affected the financial development of the country and also the livelihood of many people. Severe Acute Respiratory Syndrome Corona Virus (SARS-CoV) and Middle East respiratory Syndrome Corona Virus (MERS-CoV) are the viruses that caused respiratory issues that lead to the death of people.

Real Time Reverse Transcription Polymerase Chain Response (RT-PCR) is the extensively recognized testing method right now utilized for COVID detection. Computed Tomography(CT), X-Ray are chest radiological imaging techniques which have essential part in early recognition and treatment of this disease [2]. There are high chances of recognizing symptoms by analyzing radiological pictures of patient's regardless of whether negative outcomes are obtained from RT-PCR test. Likewise, the sensitivity of RT-PCR test is low (60 to 70%) [3]. Less number of test kits, reliability in the results are the major issues associated with the test kits. Major characteristics of Covid were seen in the chest X-Ray images even though the patient did not show any external symptoms [4]. This strengthens the importance of X-Ray images in detecting Covid virus in the patient. The characteristics of Covid that can be seen in the X-Ray images as : Bilateral Alveolar Consolidation, Ground Glass Opacities, Irregular Opacities and consolidations, Vascular dilation in the lesion, Interlobular septal thickening, vascular expansion, rounded opacities etc [5]. Figure 1 shows the Covid characteristics in X-Ray images.

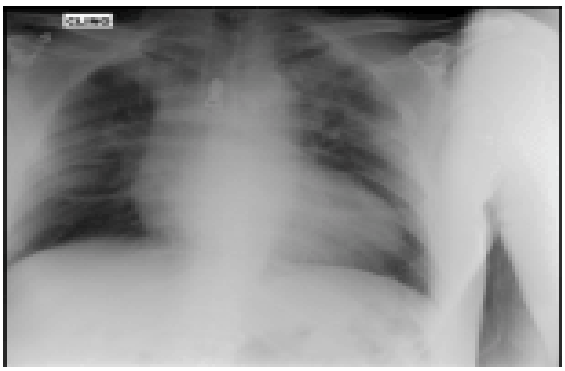

Fig. 1 (a). Bilateral Alveolar consolidations at the upper region

Fig. 1 (b). Vascular Dilation at the Lesion

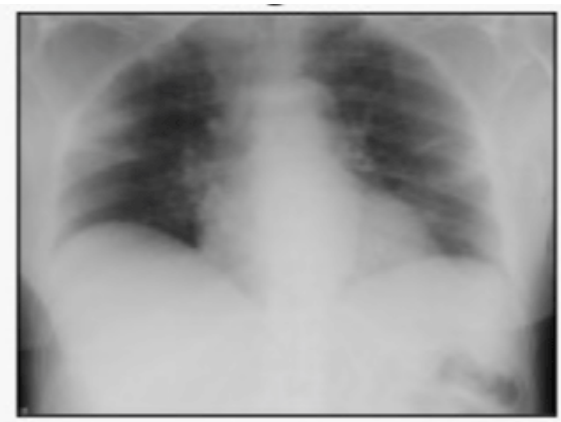

Fig. 1 (c). Ground Glass Opacities at the bottom region and corners; Vascular expansion at the center

Fig. 1 (d). Irregular Opacities and Ground Glass Consolidations

Application of DL methods for automatic detection and diagnosis of diseases has become a very useful tool for clinicians [6,7]. It helps to create end-to-end models for obtaining desired outcomes by feeding the input data without manually extracting features from the input data [8]. Computer Aided Diagnosis (CAD) give the results in less time when compared to the conventional testing techniques. In addition, there are high chances of accurate detections with the help of CAD systems. Early detection helps in speedy recovery thereby controlling the spread of virus. CAD system can overcome the low availability of conventional testing kits, and can also be taken to any far places to reduce costs and increase the number of tests conducted within a day. The major contribution of the proposed work is in decreasing the number of false positives and false negatives by feeding noise filtered X-Ray images to the DL framework. The next section briefs the related work, followed by methodology, results and discussions. Last section draws the conclusion.

A. Related Works

Deep-learning (DL) algorithms helps in designing models that can be used in many fields. DL has been utilized to make models that can recognize Covid from Chest X-Ray images [9-11]. A DL model proposed by Wong and Wang [12] for COVID19 detection (COVID-Net), gave an accuracy of 92.4%. Sethy and Behera [13] proposed a model with CNN layers and a SVM classifier to recognize Covid. Ioannis et al.[14] proposed a DL model, which utilized VGG19 Architecture to detect Covid which gave an exactness of 93.48. Ioannis D.Apostolopoulos and Tzani A. Mpesiana [15] proposed a DL framework utilizing MobileNet Architecture for Covid-19 discovery and acquired an exactness of 94.72. Antonios Makris, Konstantinos Tserpes [16] proposed diverse DL models with various structures for Covid identification. Among the various models experimented by them, the VGG16 model outperformed and acquired a maximum accuracy of 95.88%. A COVIDX-Net model having 7 CNN layers was proposed by Hemdan et al.[17] to detect and diagnose Covid. A DL model proposed by Tulin Ozrturk [18] built the model utilizing the Dark Covid-Net model and accomplishes an exactness of 87.02%. All the above proposed Deep Learning models are used to detect Covid-19 from Chest X-Ray images.

II. METHODOLOGY

A. Pre-Processing of the Dataset Images

Preprocessing of images is performed to make the data accurate for the subsequent stages. Noise filtering of images is done using linear and nonlinear filters and the performances of the filters is observed through the performance metrices to finalize the best suitable filter for the dataset images. Gaussian filter, mean filter, median filter and weiner filters were used to perform noise filtering of X-Ray images. The following performance metrics, namely Mean square error, Structure Similarity Index, Peak Signal to Noise Ratio have been calculated to observe the performance of the filters for the dataset images. As the dataset is a collection of images from different open sources, the images are of different sizes, so kernel size was adjusted according to the image size.

The Mean square error, Structure Similarity index, PSNR are calculated using the formulas below.

$$\text{MSE} = \frac{\sum_{M,N}[I_1(m,n) - I_2(m,n)]^2}{M * N} \quad (1)$$

$$\text{SSIM}(x,y) = \frac{(2\mu_x\mu_y + c_1)(2\sigma_{xy} + c_2)}{(\mu_x^2 + \mu_y^2 + c_1)(\sigma_x^2 + \sigma_y^2 + c_2)} \quad (2)$$

$$\text{PSNR}(x,y) = 10\log_{10}\left(\frac{R^2}{MSE}\right) \quad (3)$$

B. Proposed Model

VGG Architecture

The VGG16 Architecture has got 13 convolutional layers and 5 max-pool layers and 3 full connected layers. The 13 convolution

layers and 3 full connected layers are the 16 layers present in VGG16 architecture. The VGG architecture has two blocks of 2 convolutional layers after which a max-pool layer is placed. Next, three blocks of 3 convolutional layers followed by another max-pool layer. And at the end, there will be 3 layers of different depth. The deepness of the network keeps increasing from layer to layer in the architecture. At the output, there will be a softmax layer. In the architecture, a channel of size 64 is initialized, incrementing the size by a step of 2 after every max-pooling layer until the size becomes 512. Convolutional layer has a small receiving field of 3*3 and a step of 1. Row and Column padding is done in every convolutional window so that there will be uniformity in size of input and output feature maps. Max-pool activity is performed via a window of size 2*2 with a step of 2 so the maximum pooling windows are not overlapping. The initial two full connected layers have 4096 channels each. The final and the third full connected layer will have 1000 channels. The third full connected layer is the output layer. The shrouded layers have ReLU as the Activation Function. The pictorial representation of VGG16 Architecture can be seen in figure 2 and the pathway of data inside the VGG Architecture can be seen in figure 3.

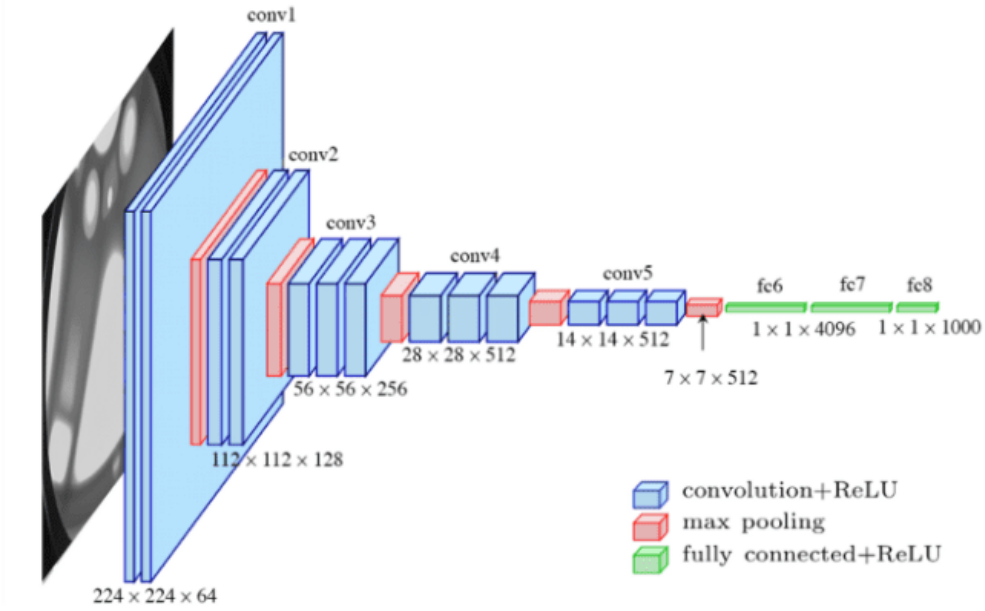

Fig 2. Architecture of VGG16

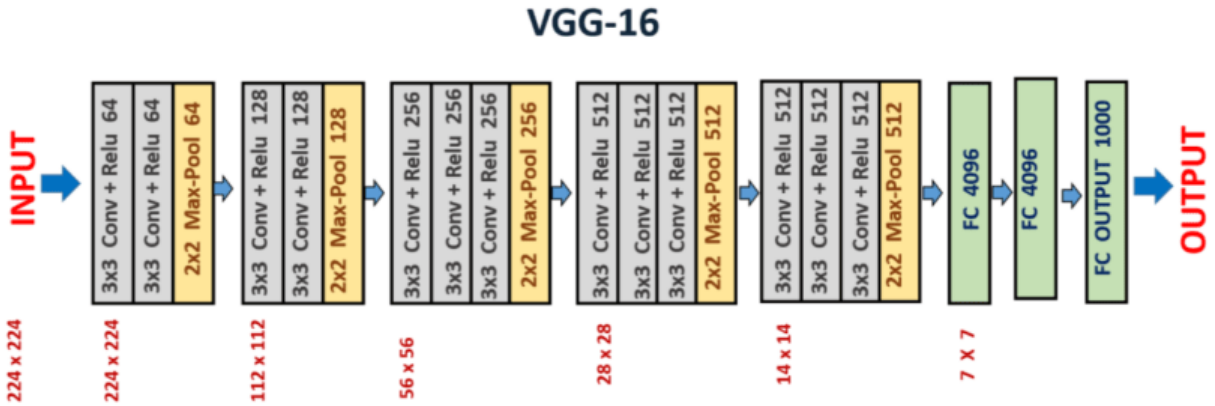

Fig. 3. The pathway of data inside the VGG16 Architecture

C. *Training of the Model*

The noise filtered images are divide into two sets and labelled as train set and test set. The images present in test set are labelled as C(Covid), P(Pneumonia), N(Normal). Data Augmentation has been performed for compensating the scarcity of medical images. Normalisation and scaling of dataset images is done to maintain uniformity of dataset images pixel wise. Vertical flip is done to set the images which might be stored upside down. The images are then passed

through the VGG16 model to carry out the training of the model. The images will be split into batches and will be passed through the model multiple times as a part of training process. The number of iterations and batch size can be varied by the user. Inorder to enhance the generalization performance of the model, fivefold cross-validation was employed. To assess the reliability of the proposed deep learning model which detects COVID-19, various performance metrics like F1 Score, precision, accuracy, recall are computed. The testing is done for the noise filtered dataset images and also for the same dataset image without performing noise filtering to check the importance of the pre-processing step in reducing the number of false detections and the output results are recorded.

III. RESULTS

A. Pre-Processing of Dataset Images

The first step is performing noise filtering of the dataset images using Gaussian, Weiner, Mean and Median filters and to find the appropriate filter for the dataset images. Figure 4 and 5 shows a sample image output after filtering it using the above mentioned filters.

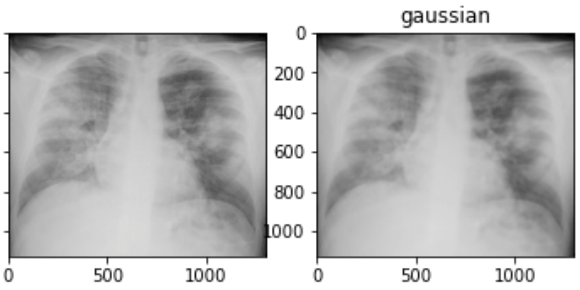

Fig. 4 (a). Outputs of first X-Ray image before and after filtering it using Gaussian Filter

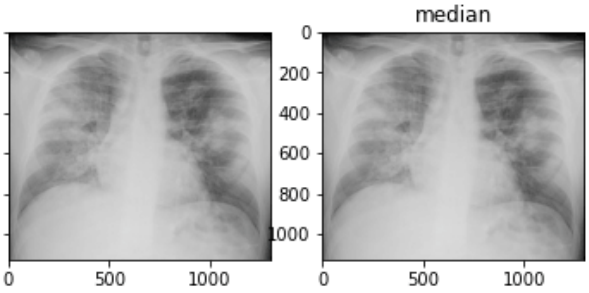

Fig. 4 (b). Outputs of first X-Ray image before and after filtering it using Median Filter

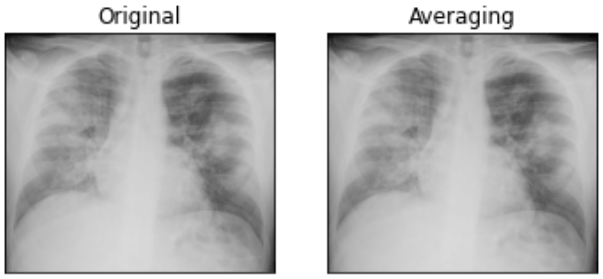

Fig. 4 (c). Outputs of first X-Ray image before and after filtering it using Mean Filter

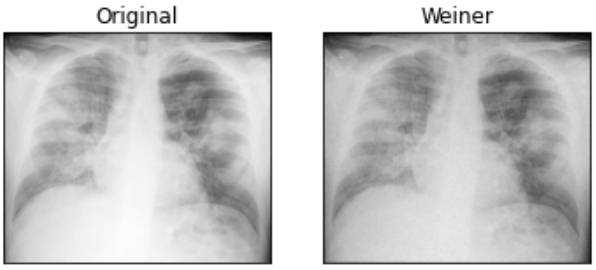

Fig. 4 (d). Outputs of first X-Ray image before and after filtering it using Weiner Filter

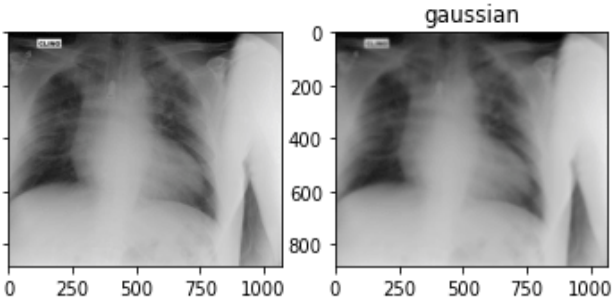

Fig. 5 (a). Outputs of second X-Ray image before and after filtering it using Gaussian Filter

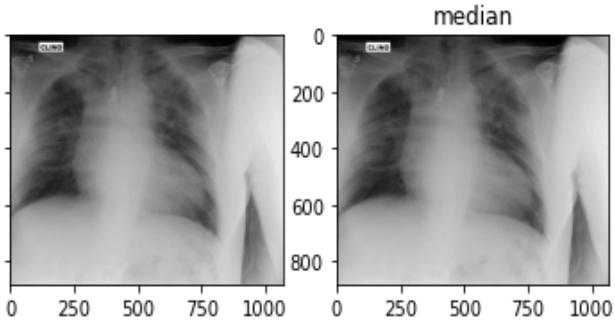

Fig. 5 (b). Outputs of second X-Ray image before and after filtering it using Median Filter

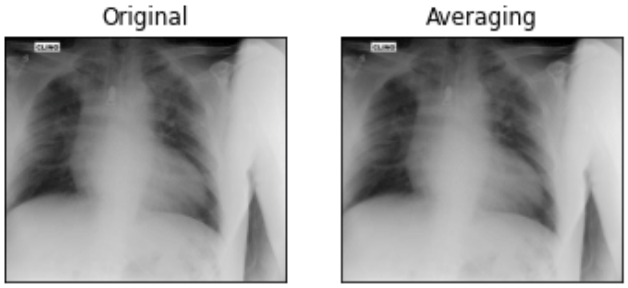

Fig. 5 (c). Outputs of second X-Ray image before and after filtering it using Mean Filter

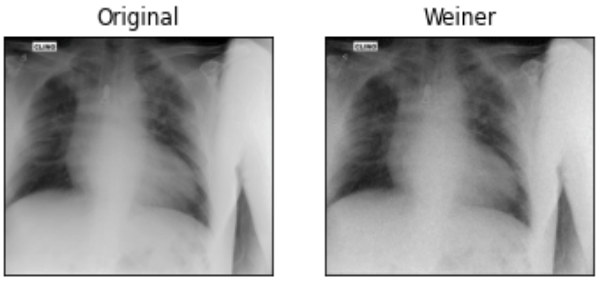

Fig. 5 (d). Outputs of second X-Ray image before and after filtering it using Weiner Filter

Table 1, Table 2, Table 3 displays the range of PSNR, MSE and SSI values obtained respectively for the dataset images after filtering through the four filters.

Table 1. Peak Signal To Noise Ratio (dB)

Gaussian	Mean	Median	Weiner
42	40	32	55
40	33	32	36
43	41	37	06
40	37	35	47
46	43	30	45
45	38	32	52
44	33	31	07

PSNR is used for measuring the quality between the original and compressed images. Higher PSNR vlue indicates good quality of the compressed or reconstructed image. Gaussian Filter has shown consistent PSNR values when compared to other filters. Also the PSNR values are in good range (40 to 50) which makes it a right choice for the dataset images.

Table 2. Mean Square Error

Gaussian	Mean	Median	Weiner
0.7566	2.3011	2.8865	5979.7602
1.2119	2.7354	2.9023	28140.2549
1.3984	3.2173	2.6170	11643.8860
1.4004	4.5219	4.3875	9550.0316
1.6743	1.8226	1.7378	15395.5156
1.1732	4.4911	3.9771	9696.8330

Mean Square Error is the average of squares of the difference of the value estimated and the true obtained value. The lower the Mean Square Error value, the better the filter for the dataset images.

Table 3. Structure Similarity Index

Gaussian	Mean	Median	Weiner
0.9946	0.9891	0.9324	0.0045
0.9915	0.9803	0.9110	0.0042
0.9836	0.9659	0.9221	0.0038
0.9843	0.9669	0.9510	0.0063
0.9807	0.9729	0.9119	0.0042
0.9815	0.9596	0.9275	0.0034

Structure Similarity Index is used for predicting the perceived quality of the dataset images. It quantifies the image quality degradation which would have happened during the filtering

process. An index value between -1 and 1 means a good performance by the filter.

The performance metrics indicates that Gaussian filter is most suitable for the dataset images than the other filters. Also the irregular size of dataset images forced to change the kernel size for each and every image. But Gaussian filter performed well for low and high kernel size and solved the need to change the kernel size repeatedly. Other filters performance was different for different kernel size but Gaussian filter gave a consistent and desirable performance for lower and higher kernel sizes.

B. Validation Testing of the Trained Model

After pre-processing the dataset images using Gaussian Filter, Validation testing is done for images with and without pre-processing to find the importance of pre-processing in reducing the number of false detections. The Confusion matrices for both the datasets obtained after validation testing are shown below:

Without Pre-processing:

EXPECTED / TRUE	NORMAL	COVID-19	PNEUMONIA
NORMAL	271	14	20
COVID-19	18	265	22
PNEUMONIA	26	23	256

With Pre-processing:

EXPECTED / TRUE	NORMAL	COVID-19	PNEUMONIA
NORMAL	297	6	2
COVID-19	9	281	15
PNEUMONIA	6	27	272

The performance matrices calculated using the Confusion Matrices are presented in table 4. Table 5 presents the false positive rates and false negative rates in all cases. Table 6 compares the proposed model to the other models which were programmed for Covid detection from X-Ray images. The scheme presented shows that the proposed model with pre-processing outperforms the state-of-the-art models without pre-processing. The pre-processing incorporated justifies the merit of proposed approach in reducing the false positives and false negatives.

TABLE 4. Performance metrics calculated using Confusion Matrices

STATS	WITHOUT PRE-PROCESSING			WITH PRE-PROCESSING		
	COVID	NORMAL	PNEUMONIA	COVID	NORMAL	PNEUMONIA
PRECISION	0.89	0.95	0.94	0.90	0.96	0.95
RECALL	0.92	0.97	0.89	0.94	0.98	0.90
F1 SCORE	0.91	0.96	0.92	0.92	0.97	0.92
ACCURACY	**92.98%**			**96.56%**		

TABLE 5. False Positive Rates and False Negative Rates calculated for all the cases

FALSE RATES	WITHOUT PRE-PROCESSING			WITH PRE-PROCESSING		
	COVID	NORMAL	PNEUMONIA	COVID	NORMAL	PNEUMONIA
FALSE POSITIVE RATE	0.072	0.07	0.06	0.024	0.03	0.05
FALSE NEGATIVE RATE	0.100	0.16	0.13	0.026	0.10	0.08
OVERALL FALSE POSITIVE RATE	**0.067**			**0.034**		

TABLE 6. Comparison of the proposed model to the other DL models which are programmed for Covid-19 detection from X-Ray images

References	**Type of Radiological images**	**Architecture**	**Accuracy**
Ioannis et al.[14]	X-Ray images	VGG19	93.48%
Sethy and Behra[13]	X-Ray images	ResNet50 and SVM	95.35%
Wang and Wong[12]	X-Ray images	COVID-Net model	92.4%
Hemdan et al.[17]	X-Ray images	COVIDXNet	89%
Ioannis D.Apostolopoulos and Tzani A. Mpesiana[15]	X-Ray images	MobileNet	94.72%
Tulin Ozturk[18]	X-Ray images	Dark CovidNet model	87.02%
Antonios Makris, Konstantinos Tserpes[16]	X-ray images	VGG16 VGG19 XCeption	95.88% 95.03% 76.47%
Proposed model	**X-Ray images**	**VGG16**	**96.56%**

IV. CONCLUSION

In this study, a fully automated deep learning based model is proposed to detect imperfections from X-Ray images. The model will treat a perfect image as normal condition. This model is an and end-to-end structure which doesn't need the extract features manually. The model is giving an accuracy of 96.56. The accuracy increased from 92.98 to 96.56 because of the pre-processing performed for the dataset images. The improved reduction in the number of false positives and false negatives depicts the merit of proposed approach. The model is developed and tested using the real life X-Ray images and hence it can help in the real life purposes to detect Covid from the chest X-Ray images accurately with low cost and in short time period than the Conventional Covid testing methods.

References

[1]. F. Wu, S. Zhao, B. Yu, et al., A new coronavirus associated with human respiratory disease in China, Nature 579 (7798) (2020) 265–269.

[2]. Zu, Zi Yue, et al. "Coronavirus disease 2019 (COVID-19): a perspective from China." *Radiology* 296.2 (2020): E15-E25.)

[3]. Kanne, Jeffrey P., et al. "Essentials for radiologists on COVID-19: an update—radiology scientific expert panel." (2020): E113-E114.

[4]. S.H. Yoon, K.H. Lee, et al., Chest radiographic and CT findings of the 2019 novel coronavirus disease (COVID-19): analysis of nine patients treated in Korea, Korean J. Radiol. 21 (4) (2020) 494–500.

[5]. H. Anandakumar and K. Umamaheswari, "A bio-inspired swarm intelligence technique for social aware cognitive radio handovers," Computers & Electrical Engineering, vol. 71, pp. 925–937, Oct. 2018. doi:10.1016/j.compeleceng.2017.09.016

[6]. R. Arulmurugan and H. Anandakumar, "Early Detection of Lung Cancer Using Wavelet Feature Descriptor and Feed Forward Back Propagation Neural Networks Classifier," Lecture Notes in Computational Vision and Biomechanics, pp. 103–110, 2018. doi:10.1007/978-3-319-71767-8_9

[7]. Haldorai, A. Ramu, and S. Murugan, "Social Aware Cognitive Radio Networks," Social Network Analytics for Contemporary Business Organizations, pp. 188–202. doi:10.4018/978-1-5225-5097-6.ch010

[8]. R. Arulmurugan and H. Anandakumar, "Region-based seed point cell segmentation and detection for biomedical image analysis," International Journal of Biomedical Engineering and Technology, vol. 27, no. 4, p. 273, 2018.

[9]. Tamuly, Sudarshana, C. Jyotsna, and J. Amudha. "Deep Learning Model for Image Classification." *International Conference On Computational Vision and Bio Inspired Computing*. Springer, Cham, 2019.

[10]. Rajkumar, A., M. Ganesan, and R. Lavanya. "Arrhythmia classification on ECG using Deep Learning." 2019 5th International Conference on Advanced Computing & Communication Systems (ICACCS). IEEE, 2019.

[11]. Haritha, H., and Senthil Kumar Thangavel. "A modified deep learning architecture for vehicle detection in traffic monitoring system." *International Journal of Computers and Applications* (2019): 1-10.

[12]. L. Wang, A. Wong, COVID-Net: A Tailored Deep Convolutional Neural Network Design for Detection of COVID-19 Cases from Chest Radiography Images, 2020 arXiv preprint arXiv:2003.09871.

[13]. P.K. Sethy, S.K. Behera, Detection of Coronavirus Disease (COVID-19) Based on Deep Features, 2020.

[14]. Ioannis D. Apostolopoulos1, Tzani Bessiana, COVID-19: Automatic Detection from X-Ray Images Utilizing Transfer Learning with Convolutional Neural Networks, arXiv:2003.11617.

[15]. Apostolopoulos, Ioannis D., and Tzani A. Mpesiana. "Covid-19: automatic detection from x-ray images utilizing transfer learning with convolutional neural networks." *Physical and Engineering Sciences in Medicine* 43.2 (2020): 635-640.

[16]. Makris, Antonios, Ioannis Kontopoulos, and Konstantinos Tserpes. "COVID-19 detection from chest X-Ray images using Deep Learning and Convolutional Neural Networks." *11th Hellenic Conference on Artificial Intelligence*. 2020.

[17]. E.E.D. Hemdan, M.A. Shouman, M.E. Karar, COVIDX-Net: A Framework of Deep Learning Classifiers to Diagnose COVID-19 in X-Ray Images, 2020 arXiv preprint arXiv:2003.11055.

[18]. Ozturk, Tulin, et al. "Automated detection of COVID-19 cases using deep neural networks with X-ray images." *Computers in biology and medicine* 121 (2020): 10379.